CONTROL OF THE RADIAL MOTION OF A SELF-PROPELLED MICROBOAT THROUGH A SIDE RUDDER

*L. Qiao, D. Xiao, F.K. Lu and C. Luo
Mechanical and Aerospace Engineering, University of Texas at Arlington, Arlington, TX, USA

ABSTRACT

Similar to macroboats, microboats can be potentially employed to transport a target from one place to another in a microfluidic system for the purposes of delivery and detection. In our previous works [1-3], we had developed a type of self-propelled microboats, which were capable of having straight motions at speeds of order 0.1m/s. In this work, using a combination of theoretical, numerical and experimental investigations, we explored another type of self-propelled microboats that could radial motions. This type of microboats had side rudders, and the radii of their radial motions could be controlled by varying the lengths of the side rudders.

KEYWORDS

Microboats, radial motions, rudders.

INTRODUCTION

Surface tension gradients may cause movements of a floating solid fragment on a liquid surface. These surface tension-driven motions of liquids and solid fragments are so-called Marangoni effect [4]. In the past 15 years, this effect has been applied to drive gels, whose dimensions ranged from millimeter to centimeter scales [5-7]. A gel was firstly immersed in a liquid (such as ethanol) and then placed in water. This liquid had a lower surface tension than water. Once it was expulsed from the gel, the surface tension difference between water and the liquid made the gel have translational and rotational motions. These motions depend on the size, shape, symmetry, and spouting hole of a gel. The gel of a smaller size might move faster [5]. Disk- [5-6] or rectangular-shaped gels [7] mainly had translational motions, while cubic- [7] or Y-shaped gels [7] had rotational motions. Our group also developed mm-scale SU-8 microboats and microflotillas using Isopropyl alcohol (IPA) as the propellant [1-3], which were capable of having translational motions along the longitudinal directions at the speeds of order 0.1 m/s. In this work, we further investigated how to steer the microboat in an open water area. For this purpose, we incorporated rudders of various lengths into the right sides of microboats, and explored the effects of these rudders on the radial motions of the microboats using a combination of theoretical, numerical and experimental investigations.

PROPULSIVE MECHANISM

As shown in figure 1, the propulsion of a microboat on a water surface was due to the difference between fore-to-aft surface tensions ($\sigma_i < \sigma_w$). When a liquid, which had a surface tension lower than water, exited the rear of the boat and covered the stern, surface tension behind the boat was reduced, becoming lower than that in front of the boat. This difference in surface tensions propelled the boat forward along its longitudinal direction.

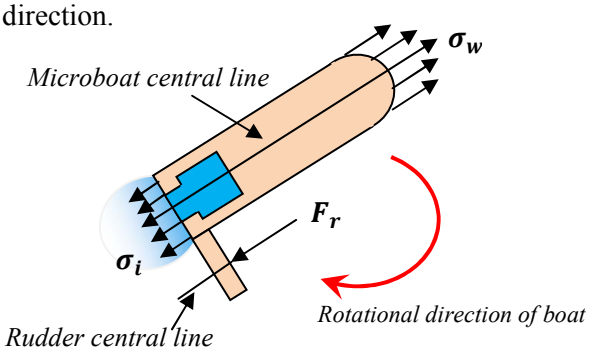

Figure 1: Force analysis of a microboat. σ_w and σ_i are surface tensions before and after the boat, respectively, and Fr is water resistance on the side rudder.

IPA was also used as the propellant in this work. There is a large difference between surface tensions of IPA and water, which are, respectively, 22.8 mN/m and 72.8 mN/m at 20 °C. The presence of a side rudder induced an additional water resistance, F_r, which created a moment to rotate the microboat. Consequently, the microboat was able to have a radial motion. The moving path in such a motion was related to the length of the side rudder.

DESIGN AND FABRICATION

Schematic of a microboat is shown in figure 2(a). The microboat comprised two SU-8 layers. The top layer included a reservoir and a nozzle. The bottom layer sealed the bottom of the reservoir and nozzle. An SU-8 side bar, which had the same thickness as the microboat, served as a rudder.

The fabrication of such a microboat included three steps (figure 2(c)): (i) place a transparency on an S1813-coated Si wafer, spin-coat the first SU-8 layer on the transparency, and pattern the SU-8 to form the bottom layer of the boat and the bottom portion of a side rudder using UV lithography, (ii) spin-coat the second SU-8 layer on the first SU-8 film, and produce reservoirs, nozzles and the top portion of the side rudder using UV lithography, and (iii) dissolve S1813 using acetone and remove the transparency, together with the generated SU-8 microboat, from the Si wafer. Seven types of microboats were fabricated. They had the same hulls (25

mm long, 6 mm wide and 1 mm thick), while their side rudders were 2, 4, 6, 7, 8, 9 and 10 mm long, respectively. These rudders had the same widths of 2 mm and the same thicknesses of 1 mm. A representative microboat generated was given in figure 2(b). Its rudder was 2 mm long.

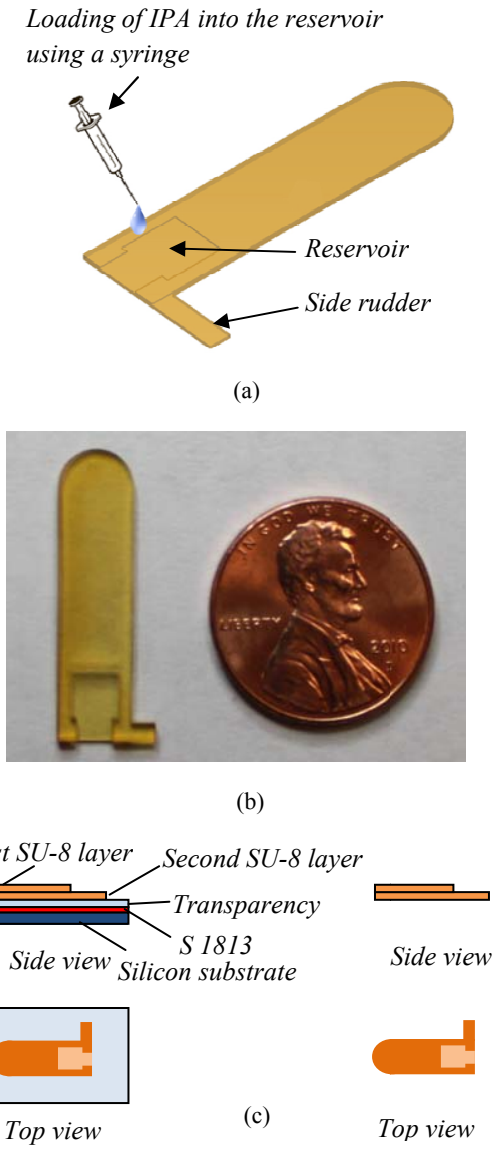

Figure 2: Schematics and fabrication process of a SU-8 microboat with a side rudder: (a) 3-D view of the SU-8 boat. A syringe with precision of 0.05 µl was use to load IPA into the reservoir in the experiments. (b) A representative microboat generated. (c) Procedure to fabricate a microboat.

TEST RESULTS AND DISCUSSIONS

Through experiments, we determined relationship between the length of a rudder and the radius of a radial motion. The radius was obtained according to the recorded moving trajectories.

Microboats were tested in a 32-cm-long and 23-cm-wide glass container, which was partially filled with 1-cm-deep distilled water. A paper marked with 1 cm x 1 cm square patterns was placed underneath the glass container to find the location of a microboat. The water was changed after each test. At the beginning of every test, 1.2 µl IPA was loaded in the reservoir of a microboat. As shown in figure 3(a), the microboat first started moving along the horizontal direction for a short time, then began to have a radial motion along approximately circular trajectories, and finally stopped. The motion was recorded by an HD digital camera (SONY HDR-XR500, frame rate: 30 fps). It was subsequently analyzed using Matlab R2010a. Each motion lasted around 20 s, and the position of the microboat was tracked every 0.1 s. Accordingly, about 200 data points were used to analyze each motion.

Figure 3 showed representative test results of microboats with 2-, 4-, and 8-mm-long rudders, respectively.

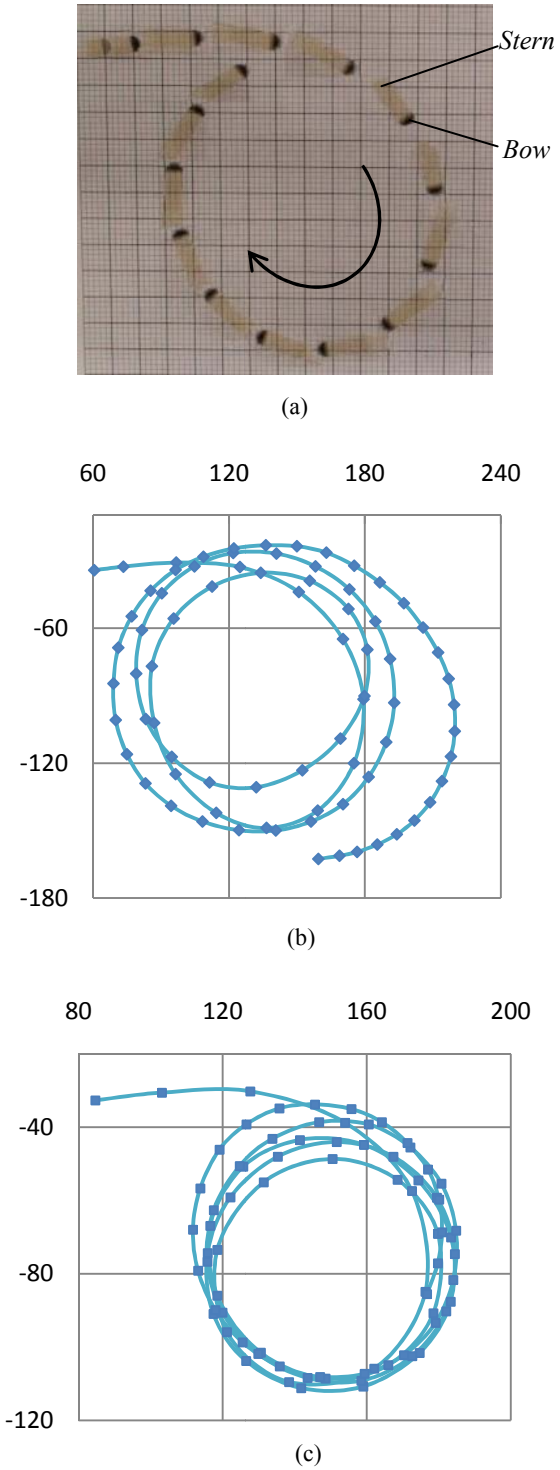

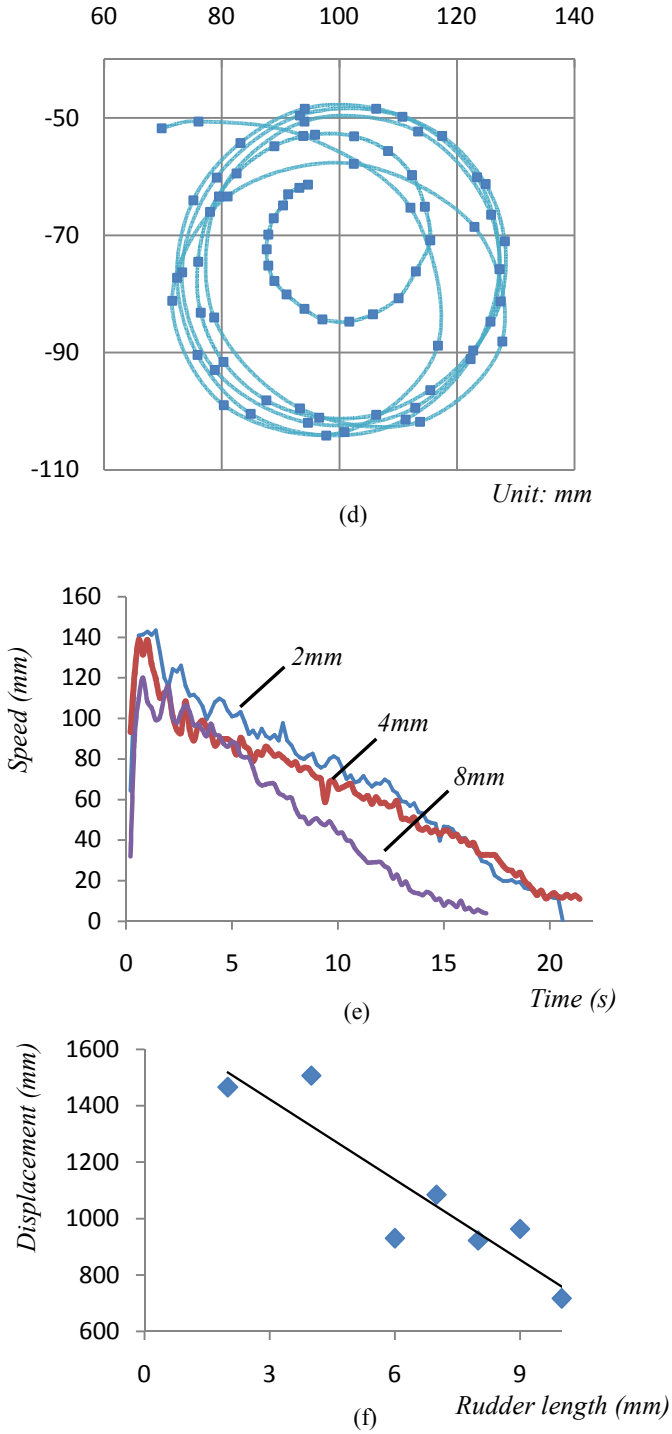

Figure 3: Experimental results (a) Sequential snapshots of a radial motion for the microboat with a 2-mm-long rudder, experimental trajectories for the microboats with (b) 2-, (c) 4-, (d) 8-mm-long rudders, (e) representative speed vs. time curves and (f) total displacement vs. rudder length.

Figure 3(a) gives sequential snapshots of the first loop in the radial motion of the microboat with the 2-mm-long rudder. After the acceleration during the first second of the motion, the speed of boat began to decreased from the maximum speed, which was around 0.14 m/s. The corresponding trajectory was close to a circle. Figures 3(b)-3(d) are complete trajectories of microboats with 2-, 4- and 8-mm-long rudders, respectively. The average radius of the approximately circular path and total travel distance both decreased with the increase in the length of the side rudder (figures 3(f) and 4(b)).

Theoretical and numerical modeling

Based on the free-body diagram shown in figure 1, the radial motion of a microboat may be described by the following three equations of motion:

$$I\frac{dw(t)}{dt} = M_{dv} - M_{dg}, \quad (1)$$

$$m\frac{dv_x(t)}{dt} = F_{dv}\cos\theta(t) - F_{xdg}, \quad (2)$$

$$m\frac{dv_y(t)}{dt} = F_{dv}\cos\theta(t) - F_{ydg}, \quad (3)$$

where I denotes the moment of inertia, m the mass of the microboat with rudder, w the angular velocity, v_x and v_y the translational speeds in x and y directions respectively, and θ the angle of rotation at that moment. In equation (1), M_{dv} and F_{dv} are the driving torque and force, which are determined by

$$M_{dv} = F_{dg}{}' \times d, \quad (4)$$

$$F_{dv} = (\sigma_w - \sigma_i)W, \quad (5)$$

where the $F_{dg}{}'$ is the drag force acting on side rudder, d is the distance between the middle lines of the microboat and the rudder (figure 1), σ_w and σ_i are the surface tensions of water and IPA, respectively, W is the width of the microboat. In the equations (1)-(3), M_{dg} is the moment induced by the drag, while F_{xdg} and F_{ydg} are the components of total drag in x and y directions, respectively. These three items, as well as $F_{dg}{}'$, can be determined by the equations,

$$M_{dg} = \int_{-\frac{L}{2}}^{\frac{L}{2}} \eta\, w(t)\, r^2\, dr \quad (6)$$

$$F_{xdg} = \eta\, v_x(t)\, W_c \quad (7)$$

$$F_{ydg} = \eta\, v_y(t)\, W_c \quad (8)$$

$$F_{dg}{}' = \eta\, v(t)\, W_r \quad (9)$$

where L is the length of the microboat, W_c is the characteristic length of boat and equals one half of the summation of boat length and width, W_r is the length of the side rudder and η is the coefficient between drag and the product of speed and object width. Because the Reynolds number in our case was around 1000, the flow around a microboat is considered to be laminar. Based on the relationship between drag coefficient C_d and Reynolds number R_e in the case that a flat plate is immersed in a laminar flow [9], we propose $C_d = \frac{\alpha}{R_e}$ where α is an unknown coefficient. C_d and R_e are also defined by the equations, $C_d = \frac{F_{dg}}{0.5\,\rho\, v^2\, w\, D}$ and $R_e = \frac{v\,D}{\upsilon}$, where ρ is water density, w width of flat plate, D the length of flat plate and υ kinematic viscosity of fluid. Accordingly, we have $F_{dg} = 0.5\,\alpha\,\upsilon\rho\, v\, w$, which indicates that drag is linearly proportional to the product of speed and plate width when water density and kinematic viscosity are constant. If we further define $0.5\,\alpha\,\upsilon\rho$ as η, we can obtain equations (6)-(9) as given above.

After plugging equations (4)-(9) to the three equations of motion (i.e., equations (1)-(3)), we find that η is the only unknown to be determined. The speeds

could be experimentally measured (figure 3(e)) According to the in-situ observation, IPA was completely consumed within around 1 s after it had started moving out of the reservoir. Thus, after first two seconds of a motion, there should be no driving force and consequently the microboat should suffer only drag forces. The total drag force could be determined by the deceleration of microboat. Subsequently, η could be calculated. Finally, the three equations of motion are solved using Matlab. The initial conditions are all set to be zero. The driving force is considered to be constant before the complete consumption of the IPA. The first moving loops that were simulated are given in figure 4 (a). Numerically and experimentally determined relationships of the radius of motion with the length of rudder were given in figure 4(b).

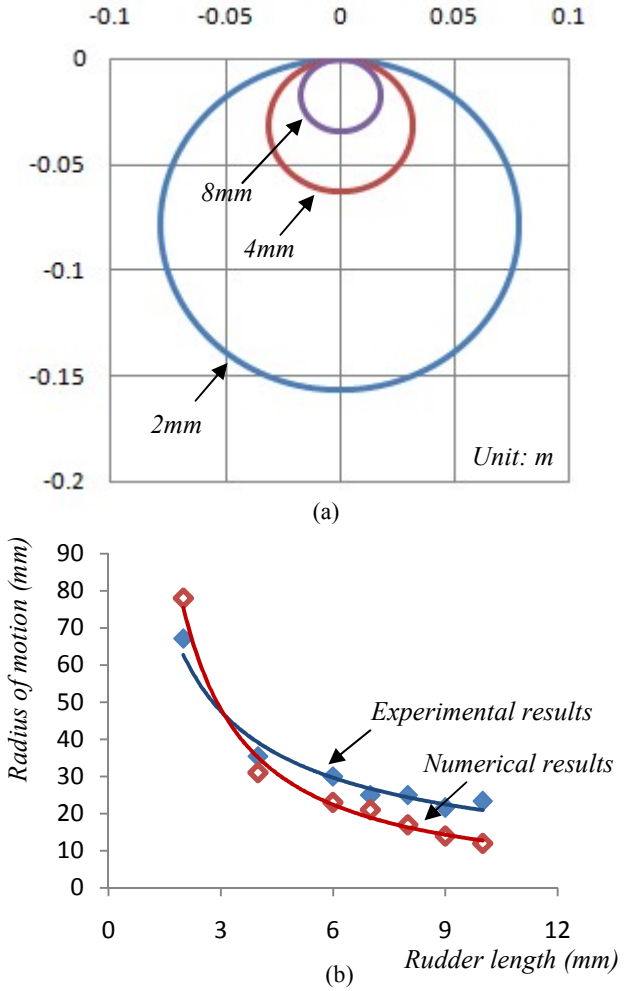

Figure 4: (a) Representatively simulated trajectories of 2-, 4-, and 8-mm-long rudders microboats. (b) The comparison between the simulated results and experimental results of radius of motion vs. rudder length.

It can be seen from figure 4(b) that, when the length of a rudder is less than 7 mm, the numerical results have a good match with those of experiments. However, with the increase in the rudder length, the simulated radius of motion became gradually smaller than the corresponding experimental value. Two issues in simulation might cause errors. First, we assumed that the IPA only covered the stern but not the rear part of the side rudder. In real situations, IPA might cover part of the side rudder. Accordingly, an opposite torque would be generated due to the difference in the surface tensions between the front and rear portions of the side rudder, causing the increase in the radius of motion. The degree of this increase increased with the length of the side rudder, making the difference between numerical and experimental results also increase with the length of the side rudder. Second, when calculating the moment induced by drag, we only consider the drag acting on the microboat and did not consider that on the rudder.

CONCLUSIONS

In conclusion, the presented experimental results demonstrate: (i) through a side rudder, it is feasible to control the radial motion of a microboat; (ii) the radius of a radial motion decreases as the length of a rudder increases; and (iii) the total travel distance and the maximum speed both decrease as the length of a rudder increases. The theoretical results show that the trajectories of the microboat motion can be obtained by solving equations of motion. When a rudder is short, the numerical results have a good match with the experimental results, while the mismatch between numerical and experimental results increased with the length of the side rudder due to the simplified consideration in the simulation.

REFERENCES:

[1] C. Luo, H. Li, and X. Liu, "Propulsion of microboats using isopropyl alcohol as a propellant", Journal of Micromechanics and Microengineering, Vol. 18, pp. 067002, 2008.

[2] C. Luo, L. Qiao and H. Li, "Dramatic Squat and Trim Phenomena of MM-Scaled SU-8 Boats Induced by Marangoni Effect", Microfluidics and Nanofluidics, Vol. 9 (2-3), pp.573-577, 2010.

[3] H. Li and C. Luo, "Development of a self-propelled microflotilla." Microsystem Technologies: (in press; available on journal website), 2011.

[4] E. Scriven, V. Sternling, "The Marangoni effects." Nature, Vol.167, pp.186–188, 1960.

[5] Y. Osada, P. Gong, M. Uchida, N. Isogai, "Spontaneous motion of amphoteric polymer gels on water", Jpn J Appl Phys, Vol. 34, pp.511–512, 1995.

[6] P. Gong, S. Matsumoto, M. Uchida, N. Isogai, Y. Osada, "Motion of polymer gels by spreading organic fluid on water", J Phys Chem, Vol.100, pp.11092–11097, 1996.

[7] N. Bassik, T. Abebe, H. Gracias, "Solvent driven motion of lithographically fabricated gels", Langmuir, Vol.24, pp.12158–12163, 2008.

[8] D. Munson, D. Young and T. Okiishi, "Fundamentals of fluid mechanics", 4th edition, John Wiley and Sons, 2002.

CONTACT

*L. Qiao, * *lei.qiao@mavs.uta.edu*